Available online at www.sciencedirect.com
ScienceDirect
International Journal of Sediment Research 25 (2010) 91-109
INTERNATIONAL JOURNAL OF SEDIMENT RESEARCH
www.elsevier.com/locate/ijsrc

Simulation of erosion-deposition processes at basin scale by a physically-based mathematical model

Pedro A. BASILE[1,3], Gerardo A. RICCARDI[1,4], Erik D. ZIMMERMANN[1,5], and Hernán R. STENTA[2,3]

Abstract

The development and application of the physically-based and spatially-distributed mathematical model CTSS8-SED is presented. The model simulates hydrologic-hydraulic processes produced by storm events and related soil erosion and sediment transport processes at basin scale in lowland areas. The model simulates (i) storm runoff, (ii) soil detachment by raindrop impact and overland flow (gross sediment yield), (iii) sediment transport by overland flow and associated erosion-deposition processes and (iv) sediment transport by stream flow and riverbed erosion-deposition processes. A quasi two-dimensional representation of water flow and sediment transport routing is made by means of interconnected cells approach. The model is applied to simulate two flooding events in the Ludueña Creek basin (Santa Fe, Argentina) occurred in April 1994 and March 2007 due to extraordinary rainfalls.

Key Words: Mathematical modeling, Erosion, Sedimentation, Ludueña Creek, Argentina

1 Introduction

Soil erosion by water plays an important role in the process of land degradation and is linked to a number of environmental and socioeconomic problems worldwide (Oldeman, 2000). The effects of water erosion can be observed both on-site and off-site (Walling and Quine, 1991; Zhou and Wu, 2008). On-site impacts are important in soils for agriculture because the disintegration of soil structure and loss of organic matter and nutrients from the upper horizons induces a decline in productivity, which leads to greater spending on fertilizers and later may cause the abandonment of agriculture (Pimentel et al., 1995; Crosson, 1997). In addition to this, off-site impacts creates different problems associated to the deposition and consolidation of sediments in reservoirs, navigation canals, storm water pipes systems, retention ponds, floodplains, etc. (Clark, 1985; Verstraeten and Poesen 1998; Khosronejad, 2009; Wang and Hu, 2009). Also, the fine sediments are likely to adsorb pollutants, such as mineral fertilizers and chemicals, which can lead to increased levels of nitrogen and phosphorus in water bodies receptors and trigger processes of eutrophication (Steegen et al., 2001; Yi et al., 2008).

In Argentina the most important soils for agricultural purposes are located on the aeolian quaternary sediments that cover the Chaco-Pampean plains. Economic losses due to on-site water erosion in the Pampean region are estimated in 700-800 million dollars/year, while for the entire nation they are estimated in 1,000-1,200 million dollars/year. However, considering all land degradation processes as well as the damages to infrastructure, losses at national level are estimated in 3,000-4,000 million dollars/year (Moscatelli and Pazos, 2000).

[1] Prof., Dr., Hydraulics Department, School of Civil Engineering, National University of Rosario, Argentina, E-mail:pbasile@fceia.unr.edu.ar
[2] Dr., Assis. Prof., Hydraulics Department, School of Civil Engineering, National University of Rosario, Argentina
[3] Research Scientist, Centre for Hydro-Environmental Research, National University of Rosario, Argentina
[4] Research Scientist, Research Council of National University of Rosario (CIUNR), Argentina
[5] Research Scientist, National Council of Scientific and Technical Research (CONICET), Argentina
Note: The original manuscript of this paper was received in Oct. 2009. The revised version was received in March 2010. Discussion open until June 2011.

The main factor contributing to the process of land degradation in Argentina is due to the intensification of agriculture in the early 70's, that is, the change from the rotation cattle-agriculture to continuous agriculture by the introduction of the double annual cropping wheat-soybean or soybean mono-cultivation and inadequate land use, partially mitigated by no-till farming started in the early 90's (Casas, 2003). Furthermore, the expansion of the agricultural frontier, mainly for soybean cropping purposes outside of the Pampean region, triggered in the last decade a dramatic deforestation rate of approximately 250,000 ha/year of native forests (UMSEF, 2007). Intensive farming and deforestation continue at present and are responsible for the increase in soil erosion, flooding risk, loss of biodiversity, sedimentation, pollution and climate change. In order to quantify water flow, sediment transport and erosion-deposition process and to evaluate remedial measures appropriated mathematical models are required.

To estimate the processes of soil erosion at basin scale mathematical models of deterministic type are usually applied. As far as the processes representation is concerned these models can be classified into empirically-based, conceptual, physically-based, or a combination of them. Depending on the time scale for which they were developed, the models can be divided into event-based and continuous. On the other hand, regarding the representation of model parameters, state variables, input, output and boundary conditions, the models can also be defined as lumped, distributed or semidistributed (Lane et al., 1988; Singh and Woolisher, 2002; Borah and Bera, 2003).

A number of watershed-scale hydrology and sediment yield models, based on the empirical USLE (Wischmeier and Smith, 1978), like AGNPS (Young et al., 1987), SWRRB (Arnold et al., 1989), RUSLE (Renard et al., 1991), SWAT (Arnold et al., 1998), AnnAGNPS (Bingner et al., 2001), have been developed. Moreover, examples of physically-based and distributed models that have been developed are ANSWERS (Beasley et al., 1980), WEPP (Foster and Lane, 1987), KINEROS (Woolisher et al., 1990), SHESED (Wicks and Bathurst, 1996), LISEM (De Roo et al., 1996), ANSWERS-2000 (Bouraoui and Dillaha, 1996), EUROSEM (Morgan et al., 1998), SHETRAN (Ewen et al., 2000), CASC2D-SED (Julien and Rojas, 2002), EROSET (Sun et al., 2002), InHM (Heppner et al., 2005), MEFIDIS (Nunes et al., 2005; 2006) and PSED (Ching-Nuo Chen et al., 2006).

Regardless the model used, no model, or group of models, will ever be appropriate for all problems and geographical situations, thus, is reasonable the continued modification of existing models and the development of new ones (Lane et al., 1988). In Argentina, very little work on the development of watershed-hydrology and sediment yield models at basin scale and its application in the Pampean region has been done. In this paper the formulation, numerical implementation and application of a physically-based and spatially-distributed computational model CTSS8-SED is presented. The model takes into consideration the relevant water flow and sediment transport mechanisms of lowland basins and is suitable to simulate storm runoff, soil detachment by raindrop impact and overland flow (gross sediment production), sediment transport by overland flow and associated erosion-deposition processes spread over the entire basin and also sediment transport by stream flow and riverbed erosion-deposition processes. Water flow and sediment processes are represented by means of interconnected cells approach in a quasi two-dimensional time-dependent numerical scheme. The model is applied to simulate two extraordinary flooding events occurred on April 03, 1994 and March 26, 2007, in the Ludueña Creek basin, located in one of the most fertile crop-field areas of Santa Fe province, Argentina.

2 Description of model formulation

2.1 Hydrologic-hydraulic processes representation

The physically-based and spatially-distributed hydrologic-hydraulic model CTSS8 (Riccardi, 2000) is based on interconnected cells approach (Cunge, 1975) and has been developed to simulate single hydrological events.

The quasi-2D continuity equation for the water flow in the j-th cell is expressed by:

$$A_j \frac{\partial z_j}{\partial t} = P_j + \sum_{k=1}^{N} Q_{j,k} \tag{1}$$

where z_j is the water level; A_j is the surface wetted area, P_j is a direct inflow into the cell (net rainfall), t is the temporal coordinate, $Q_{j,k}$ is the water discharge between cells j, and k and N is the number of cells interconnected with cell j.

Runoff abstractions can be estimated with three different algorithms based on the NRCS Curve Number Method, Horton or Green-Ampt (Chow et al., 1994). Water discharges are expressed as functions of water levels: $Q_{j,k} = Q(z_j, z_k)$; they are represented by one-dimensional discharge laws derived from the Saint-Venant dynamic equation. In the case of neglecting local acceleration and convective terms (inertia terms) we have:

$$Q_{j,k} = sign\left[z_j - z_k\right] \frac{K_{j,k}}{\sqrt{\Delta x_{j,k}}} \sqrt{\left|z_j - z_k\right|} \tag{2}$$

where $K = A_t\, h^{2/3}/\eta$ is the conveyance factor which is function of water levels in cells j and k, with A_t being the transversal wetted area between cells, η being the Manning roughness coefficient and h being the water depth; $\Delta x_{j,k}$ is the distance between the points where z_j and z_k are computed. Also, discharge laws between cells based on kinematic, quasi-dynamic and dynamic wave approximation (the last one mainly for stream flow routing) are implemented in the model for flow propagation purposes.

In order to deal with special flow conditions, weir-like discharge laws representing, levees, roads, railways embankments, etc., are also included in the model. For example, the broad weir crest formula can be used, which for free overflow weir reads:

$$Q_{j,k} = C_{q1} W_w \sqrt{2g}\ \left(z_j - z_w\right)^{3/2} \quad \text{if} \quad \left(z_k - z_w\right) < (2/3)\left(z_j - z_w\right) \tag{3}$$

and for a drowned weir:

$$Q_{j,k} = C_{q2} W_w \sqrt{2g}\ \left(z_j - z_w\right)\left(z_j - z_k\right)^{1/2} \quad \text{if} \quad \left(z_k - z_w\right) \geq (2/3)\left(z_j - z_w\right) \tag{4}$$

where z_w is the weir elevation, $C_{q1,2}$ are the discharge coefficients, g is acceleration due to gravity, W_W is the weir width and $z_j > z_k$. Equations (3) and (4) are also applied for bridges and big culverts by considering bottom step equal zero and discharge coefficient for flow through constrictions given by Ven Te Chow (1959).

2.1.1 Basin discretization and schematization of valley and river cells

The spatial distribution of model parameters and hydrological variables is done through the subdivision of the basin in cells of equal size (square grid). The cells can be specified as river-type cells or valley-type cells, the fundamental difference between the two types is related to the water storage and conveyance within the cell. In this way the basin is formed by cells that represent the areas of overland flow (valley cells) and cells that represent the stream flow (river cells).

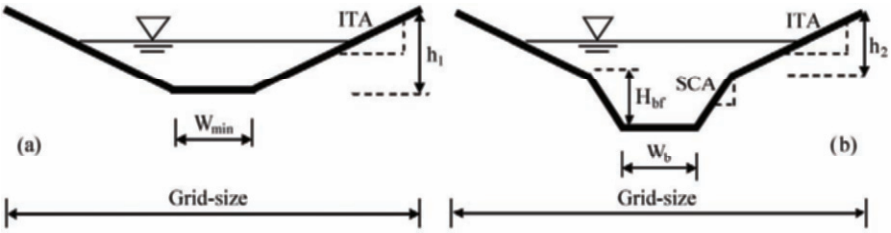

Fig. 1 (a) Geometry of valley cells, (b) geometry of river cells

The schematization of valley cells geometry is depicted in Fig. 1(a). The effective cross section for water storage and conveyance is represented by a triangular or trapezoidal section. Once grid-size is specified, the minimum width W_{min} and the transversal slope ITA define the maximum height h_1. If the water depth in the cell exceeds the maximum value h_1, the width is equal to the grid-size. In this type of cells is necessary to define the Manning roughness coefficient, the minimum width (W_{min}) and the lateral slope (ITA).

The schematization of river cells geometry is depicted in Fig. 1(b). For river cells the model allows the adoption of compounded cross sections of triangular, rectangular or trapezoidal type. The cross section is located in the center of the cell. In this case bottom width (W_b), side slopes (SCA and ITA), bankfull height (H_{bf}) and the corresponding Manning roughness coefficients for both main channel and side channels must be specified. The model is operated from a computational platform for data processing and geo-visualization developed in Windows® (Stenta et al., 2005).

2.2 Sediment processes representation

The sediment module incorporated into the CTSS8 model calculates soil detachment by raindrop impact and overland flow (gross sediment yield in valley cells); sediment transport by overland flow and associated erosion-deposition processes in valley cells and sediment transport by stream flow in river cells with corresponding erosion-deposition processes (Basile, 2007).

2.2.1 Gross sediment yield due to detachment by raindrop impact and overland flow in valley cells

The rate of soil detachment by raindrop impact is determined as a function of soil characteristics, rainfall intensity, water depth and vegetation cover; for the j-th cell we have:

$$D_{p_j} = c_{p_j} \ \alpha \ i_j^{\beta} \ \ f_{h_j} \ f_{c_j} \tag{5}$$

where D_p is the soil detachment by raindrop impact per unit area (kg/s$\cdot$m^2); c_p is the raindrop erodibility coefficient (kg$\cdot$m$^2\cdot$s^{-2})$^{-1}$; $\alpha\, i^{\beta}$ is the momentum squared for rainfall [(kg$\cdot$m$\cdot$s)^2/m$^2\cdot$s], with α and β being coefficients dependent on rainfall intensity i (mm/h) (Wicks et al., 1988); f_h is the water depth correction factor (Park et al., 1982) and f_c=1-R_{ac} is the vegetation cover correction factor, with R_{ac} being the total effective surface cover (Alberts et al., 1995).

Moreover, the rate of soil detachment due to overland flow is calculated using an equation of excess shear stress:

$$D_{f_j} = c_{f_j} \left(\frac{\tau_{b\,j} - \tau_{bc\,j}}{\tau_{bc\,j}} \right) \tag{6}$$

where D_{fj} is rate of soil detachment due to overland flow per unit area (kg/s$\cdot$m^2); c_f is overland flow erodibility coefficient (kg/s m^2); τ_{bj} is applied bottom shear stress (N/m^2); τ_{bcj} is critical shear stress (N/m^2), which for silty-loam cropland soils varies between 2 to 3.5 N/m^2 (Laflen et al., 1991; Nearing et al., 1991; Zhang et al., 2003).

2.2.2 Sediment routing in valley cells

The sediment routing associated with the overland flow field is simulated considering the transport capacity of the flow and comparing it with the amount of sediment available for transport, originated from the gross sediment yield (detachment by raindrop impact and overland flow) and sediment input from adjacent cells.

Sediment routing is performed by solving the quasi-2D sediment continuity equation, which for the j-th cell is expressed as:

$$(1-p)\,A_j \frac{\partial z_{b\,j}}{\partial t} = \sum_{k=1}^{N} Q_{s\ j,k} \tag{7}$$

where p is the sediment porosity; A_j is the total surface area; z_{bj} is the bottom level of the cell and $Q_{sj,k}$ is the effective sediment transport exchanged between cells j and k. The resolution of Eq. (7) determines the horizontal sediment fluxes and the corresponding erosion-deposition processes spread over the entire basin.

Sediment transport capacity of overland flow is calculated by means of Engelund-Hansen (1967) equation. By using Manning's resistance equation to eliminate water depth from dimensionless shear stress, the sediment transport capacity can be expressed in the following way:

$$Q_{sc} = \frac{c_t}{\eta_v^r} \ \frac{Q^z \ S^x}{B^y \ d^w} \tag{8}$$

where Q_{sc} is sediment transport capacity of overland flow (m^3/s), Q is the water discharge (m^3/s), S is the water surface slope (-), B is the sediment transporting width (m), d is the sediment diameter (m), η_v is the Manning roughness coefficient of valley cells (m$^{-1/3}$s), c_t is a proportionality coefficient (m$^{-1/2}$s) and the exponents are equal to: z=1.7, x=1.65, y=0.7, w=1 and r=0.3. The structure of Eq. (8) is similar to that proposed by Di Silvio (1983).

2.2.3 Sediment routing in river cells

Sediment routing processes by the stream flow are represented by the continuity equation of suspended sediment. Neglecting horizontal diffusion, the equation for the j-th cell reads:

$$\frac{\partial V_{s\,j}}{\partial t} + \sum_k Q_{sr\;j,k} + A_j\,\phi_{d\,j} - A_j\,\phi_{e\,j} = \sum_k Q_{sv\;j,k} \tag{9}$$

where V_s is the suspended sediment volume in the cell (m^3), V_s=V_w C_s, with V_w being the water volume in the cell (m^3) and C_s being the volumetric sediment concentration (m^3/m^3); Q_{sr} is the sediment transport in river cells (m^3/s), Q_{sv} is the sediment input from adjacent valley cells (m^3/s) and ϕ_d and ϕ_e the sink/source terms for deposition and entrainment of sediment respectively (m/s).

The downward vertical flux of fine sediments (deposition rate) ϕ_d is expressed as:

$$\phi_d = P\,w_s\,C_s \tag{10}$$

where P is the probability of deposition; w_s is the fall velocity of suspended sediment particle (m/s), calculated by means of Stokes law: $w_s = (s-1)g\,d^2/18\,\nu$, with s being the specific gravity of sediment (dimensionless), g being the acceleration of gravity (m/s^2), d being sediment diameter (m) and ν being the kinematic viscosity (m^2/s). The probability P of particle remaining deposited is given by Krone et al. (1977):

$$P = \begin{cases} 1 - \dfrac{\tau_b}{\tau_{cd}} & ; \quad \tau_b < \tau_{cd} \\ 0 & ; \quad \tau_b \geq \tau_{cd} \end{cases} \tag{11}$$

where $\tau_b = \rho g h S$ is the applied bed shear stress (N/m^2) and τ_{cd} is the critical bed shear stress for deposition (N/m^2).

The upward vertical flux of fine sediments (entrainment or re-suspension rate) ϕ_e is calculated with the formula proposed by Ariathurai and Arulanandan (1978):

$$\phi_e = \begin{cases} E\left(\dfrac{\tau_b}{\tau_{ce}} - 1\right) & ; \quad \tau_b > \tau_{ce} \\ 0 & ; \quad \tau_b \leq \tau_{ce} \end{cases} \tag{12}$$

where E is the erosion parameter (m/s) and τ_{ce} is critical bed shear stress for re-suspension (N/m^2).

2.3 Model applicability and calibration parameters

The model is capable to simulate spatially-distributed water flow and sediment processes with quasi two-dimensional features. The model is appropriated for lowland basins where the hydrographic network is formed by ephemeral and permanent shallow channels incised in cohesive soils. In these basins, typical of the Pampean plains of Argentina, the runoff propagation and inundation areas evolve gradually during storm events. The quasi two-dimensional flow dynamics representation is suitable because when the channels are overflowed the dynamics of runoff in valley areas takes predominantly two-dimensional horizontal features and evolve fairly slowly in time. This hydraulic behavior is totally compatible with the hypothesis on which the quasi two-dimensional models are based (Cunge, 1975; Cunge et al., 1980). On the other hand, the consideration of diffusive wave approximation to the full Saint Venant dynamic equation allows the simulation of backwater effects, which are crucial in lowland basins with strong human interference like roads embankments, railways embankments, culverts, bridges, flood detention dams, etc.. The overland and stream flows are controlled by the values of Manning roughness coefficients specified to valley and river cells and also by the discharge coefficients specified to the weir-like discharge laws. Thus, these parameters can be adjusted (between plausible limits) to reproduce discharge measurements in the hydrographic network and also to reproduce water extent inundations patterns in the entire basin.

As far as sediment is concerned, in valley cells only surface erosion by raindrop impact and overland flow is considered. The model is appropriated for soil textures characterized by different percentages of very fine sand, silt and clay. In the water stream only deposition or re-suspension of fine sediments is simulated, neither bed nor bank erosion are considered. In the valley cells, the gross sediment yield is controlled by the values of the raindrop impact (c_p) and overland flow (c_f) erodability coefficients.

Moreover, sediment transport and erosion/deposition in valley cells, as well as sediment input to the hydrographic network are controlled by the proportionality coefficient (c_t) of the sediment transport equation. It may be noted that if sediment yield measurements in the basin and suspended sediment transport data in the stream network are available, such coefficients can be regarded as calibration parameters and adjusted to reproduce sedigraphs and erosion-sedimentation maps. In ungauged basins is advisable to specify values of the erodability coefficients, usually encountered in literature, according to the textural characteristics of the soils.

3 Description of the numerical model

3.1 Water flow processes

Water flow equations are solved by finite difference approximations. The quasi two-dimensional continuity equation is discretized as:

$$A_j^n \frac{\Delta z_j}{\Delta t} = P_j^n + \theta \sum_{k=1}^{N} Q_{j,k}^{n+1} + (1-\theta) \sum_{k=1}^{N} Q_{j,k}^{n} \tag{13}$$

Developing the water discharge in Taylor series around time level $n\Delta t$, and neglecting higher order terms, we have:

$$Q_{j,k}^{n+1} = Q_{j,k}^{n} + \frac{\partial Q_{j,k}^{n}}{\partial z_j} \Delta z_j + \frac{\partial Q_{j,k}^{n}}{\partial z_k} \Delta z_k \tag{14}$$

Considering θ=1 and replacing Eq. (14) in Eq. (13) we obtain a system of M linear algebraic equations for the unknowns water levels variations Δz_j, j=1,2,…., M; with M being the total number of model cells:

$$A_j^n \frac{\Delta z_j}{\Delta t} = P_j^n + \sum_{k=1}^{N} Q_{j,k}^{n} + \sum_{k=1}^{N} \frac{\partial Q_{j,k}^{n}}{\partial z_j} \Delta z_j + \sum_{k=1}^{N} \frac{\partial Q_{j,k}^{n}}{\partial z_k} \Delta z_k \tag{15}$$

The system is closed with the corresponding upstream and downstream boundary conditions. Upstream boundary conditions can be water discharge or water level as function of time and a relationship between discharge and water level at the downstream end of the model domain. Initial conditions are represented for water levels in all cells.

For the resolution of the equations an implicit scheme is used, a numerical algorithm based on the method of Gauss-Seidel is applied. At each time step the matrix is solved and the water levels variations Δz_j for each cell are calculated. Then water levels in the center of each cell are determined as:

$$z_j^{n+1} = z_j^n + \Delta z_j \tag{16}$$

Moreover, with the discharge Eqs. (2) or (3)-(4) the flow rates $Q_{j,k}$ at time level $(n+1)\Delta t$ between the interconnected cells are calculated. Figure 2 shows the structure of square grid finite difference and the point of calculation of water levels z and discharges Q.

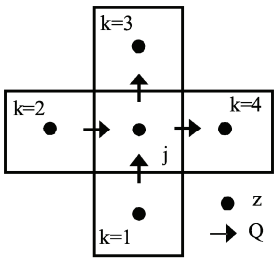

Fig. 2 Square grid finite difference schematization

Also, from the calculated water levels and discharges, other hydraulic variables like water depth at the center of the cell, transversal wetted area and hydraulic radius between interconnected cells and flow velocity in the middle point between cells linkages are calculated.

3.2 Sediment processes

The resolution procedure for the j-th valley cell can be described briefly in the following steps:

a) Rates of soil detachment by raindrop impact (D_p) and overland flow (D_f) are calculated by using Eqs. (5) and (6) respectively.

b) Sediment transport capacity (Q_{sc}) is estimated with Eq. (8) by considering an arithmetic mean diameter, which is a function of the textural characteristics of the soil.

c) Sediment continuity, Eq. (7), is solved and erosion (or sedimentation), in terms of volume variation of soil, is calculated assuming that the output sediment transport from each cell is at capacity. It is a potential erosion (or sedimentation) process, ΔV_{sp} (m^3):

$$\Delta V_{s\,pj} = A_j\,\Delta z_{b\,pj} = \frac{\Delta t}{(1-p)}\sum_k Q_{sc\,j,k} \tag{17}$$

d) The availability of sediment to be transported, in terms of volume of soil (V^*_{sdj}) is calculated. This is the sum of the accumulated sediment volume at time level nΔt (V^n_{sj}) and the gross sediment production by raindrop impact and overland flow in the same time interval Δt (ΔV_{sd} expressed in (m^3)):

$$V^*_{sd_j} = V^n_{s_j} + \Delta V_{s\,d_j} \tag{18}$$

$$\Delta V_{s\,d_j} = A_j\,\Delta z_{b\,d_j} = A_j\,\frac{\left(D_p + D_f\right)_j}{\gamma_s\,(1-p)}\,\Delta t \tag{19}$$

where, Δz_b is the bottom level variation and γ_s is the specific weight of sediments.

e) A comparison between the potential volume variation of soil and the volume of sediment available in the cell is made, distinguishing the following cases:

e_1) $\Delta V_{sp} > 0$ (sedimentation) or $V^*_{sd} > \Delta V_{sp}$: The solid discharge is not limited by the availability of sediment but by the transport capacity. The assumption that output sediment transport rates from each cell is at capacity was correct. Thus, the volume variation of soil in the cell (erosion or sedimentation) is equal to the potential volume variation of soil:

$$\Delta V_{s\,j} = \Delta V_{s\,p\,j} \tag{20}$$

The sediment volume in the cell and the effective sediment transport rates are:

$$V^{n+1}_{s_j} = V^*_{sd_j} + \Delta V_{s\,j} \tag{21}$$

$$Q_{s\;\,j,k} = Q_{sc\;j,k} \tag{22}$$

e_2) $V^*_{sd} < \Delta V_{sp}$: Sediment transport capacity can not be satisfied. Thus, the solid discharge is limited by sediment availability in the cell. In this case, the soil volume variation consists in the erosion of the total amount of available sediment:

$$\Delta V_{s\,j} = V^*_{sd_j} \tag{23}$$

$$V^{n+1}_{s_j} = V^*_{sd_j} - \Delta V_{s\,j} = 0 \tag{24}$$

The effective sediment transport rates are obtained from the quasi-2D sediment continuity equation. In fact, considering that:

$$\Delta V_{s\,p\,j} = \frac{\Delta t}{(1-p)}\sum_k Q_{sc\;j,k} \tag{25}$$

$$V^*_{sd_j} = \frac{\Delta t}{(1-p)}\sum_k Q_{s\;j,k} \tag{26}$$

Combining Eqs. (25) and (26) we obtain:

$$\sum_k Q_{s\;j,k} = \frac{V^*_{sd_j}}{\Delta V_{s\,p\,j}}\sum_k Q_{sc\;j,k} \tag{27}$$

That is, the effective sediment transport rates are proportional to the original sediment transport capacities. Bottom level in valley cells are not updated because erosion/deposition processes and the corresponding bottom level variations at basin scale during a storm event are so small that do not affect hydraulic parameters.

Sediment routing in river cells is performed by solving the continuity equation for suspended sediments, which is discretized in the following way:

$$\left(C_s V_w\right)_j^{n+1} - \left(C_s V_w\right)_j^n + \theta \sum_k \left(C_s Q\right)_{r\,j,k}^{n+1} \Delta t + \left(1-\theta\right) \sum_k \left(C_s Q\right)_{r\,j,k}^{n} \Delta t + A_j^n \left(\phi_{dj}^n - \phi_{ej}^n\right) \Delta t = \sum_k Q_{sv\,j,k}^{\;n} \; \Delta t \qquad (28)$$

where θ is a weighting coefficient ($0.5<\theta<1$) and the other variables have already been defined.

For the resolution of the equations an implicit scheme is used. At each time step the matrix is solved and the volumetric sediment concentration C_s along with sediment transport in river cells ($Q_s=C_sQ$) are calculated.

4 Model application

4.1 Brief description of the study area

The Ludueña Creek basin is located in the southern part of Santa Fe province (Argentina) (Fig. 3). Its network of permanent courses has a length of approximately 110 km. The channels are incised in cohesive soils highly resistant to erosion and capable to resist bed shear stresses of about 37 N/m^2, induced by the stream flow during short duration floods (Riccardi et al., 2005), in addition, massive bank erosion processes are negligible (Basile et al., 2005). The catchment area is approximately 700 km^2, covering one of the most fertile crop-field areas of Argentina. The mean annual precipitation is 1,000 mm. The average slope of the main stream is approximately of 0.0013 (1.3 ‰). The upper layers of soils in the watershed can be classified as silty-loam, with average percentages of very fine sand around 6%, 21% of clay and 73% of silt; the average percentage of organic matter is 2% (Zimmermann et al., 2008). The base flow rate is 0.5 m^3/s and the mean annual discharge is 2.7 m^3/s, with peak discharge of 400 m^3/s observed at Circunvalación Bridge during the extraordinary flood of 1986.

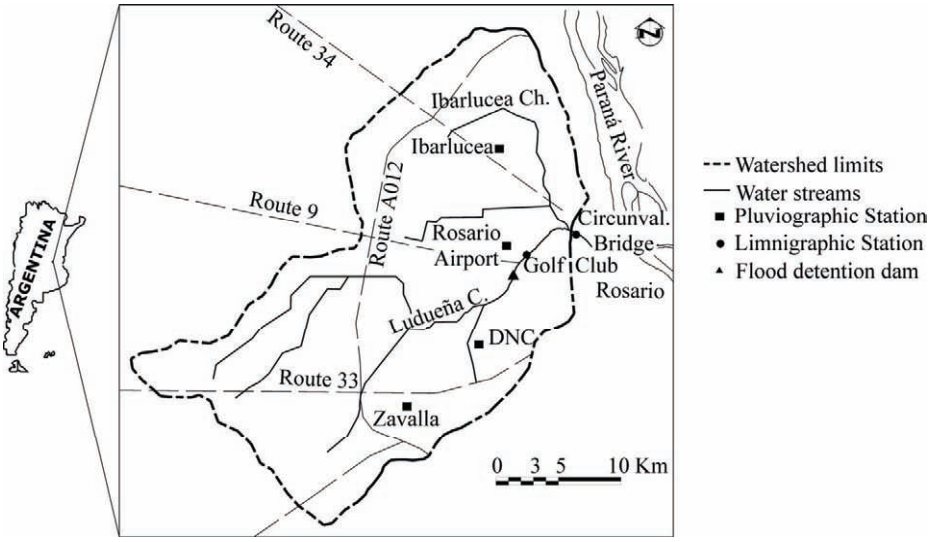

Fig. 3 Watershed of Ludueña Creek, Argentina

The basin presents a series of human interventions such as roads and railway embankments, culverts, bridges, etc., also a flood detention dam is located in the lower part of the basin, near Rosario, which became operational in 1995. The control section is located at Circunvalación Bridge in the city of Rosario. Near the Circunvalación Bridge the Ludueña Creek receives the input from the Ibarlucea channel, whose drainage area is approximately 240 km^2. Downstream of Circunvalación Bridge the Ludueña Creek crosses densely populated areas of Rosario to discharge in the Paraná river. In the urban part the stream is piped along a 1.5 km reach by means of 5 large underground conduits whose overall discharge capacity is approximately 285 m^3/s. The conduits system serves as a sort of dam, spontaneously regulated by water levels fluctuations in the Paraná river, which induces deposition of part of the transported sediments.

4.1.1 Suspended sediment transport at Circunvalación Bridge

The sediment discharge consists entirely of fine sediment (d<62.5 μm) carried in suspension as a wash load. A series of measurements at Circunvalacion Bridge were made during the years 2006-2007. Water levels were recorded and discharges were obtained from a stage-discharge curve; suspended sediments samples were taken with a point sampler and processed at lab. The concentrations of suspended sediments measured at Circunvalación Bridge, ranged from 10 ppm to 750 ppm by weight. Figure 4 shows the relationship between suspended sediment transport rate and water discharge at Circunvalacion Bridge. It is observed the usual dispersion and poor correlation between water discharge and wash load.

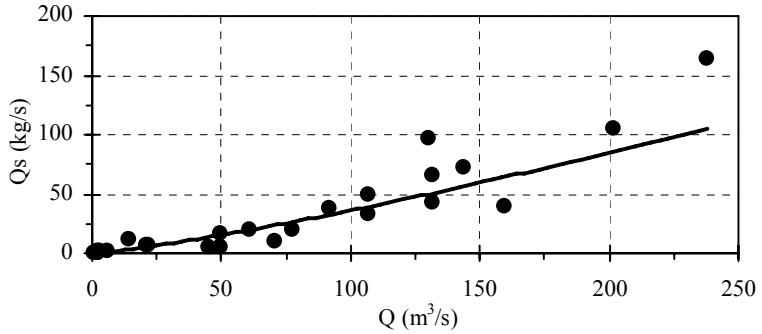

Fig. 4 Suspended sediment transport as a function of water discharge at Circunvalación Bridge

4.2 Model simulation I: Event of April 1994

The model was used to simulate a flood event and the erosion-sedimentation processes caused by an extraordinary rainfall occurred in April 1994. On that date the flood detention dam was not yet in operation. The total average precipitation in the basin was 156 mm, with a corresponding net rainfall of 106 mm and a maximum discharge of 200 m^3/s measured at Circunvalación Bridge. To implement the model rainfall data from three pluviographic stations in the basin: Rosario Airport, National Load Dispatch (DNC) and Ibarlucea were used. Also, discharge data of Ludueña Creek at Golf Club and at Circunvalación Bridge stations were available. Figure 3 shows the location of the different stations in the basin. To constitute the model different topological and spatial discretizations were tested in order to search the best attainable level of detail with the available information, especially considering the roads and railways embankments, bridges and culverts dimensions, main channels and ephemeral channels dimensions and the runoff dynamics observed in historical floods. The digital elevation model was constructed using topographic information of elevation curves spaced every 2.5 m and once the basin was spatially discretized, the bottom levels of the cells and geometry of valley and river cells were determined. The values of ITA=0.009 and W_{min}= 0.10 m were specified. The basin was discretized with squared grid-size cells of 1,000 m, a total of 779 cells with 1,473 links between cells were constituted. In Fig. 5 the basin discretization and topography for 1,000 m squared grid-size and the spatial distribution of local slopes are shown.

In the control section of Circunvalación Bridge the downstream boundary conditions was specified by means of a water level-discharge curve. Test runs were performed in order to check the correct functioning of the model. Flow continuity, wave celerity, eventual numerical instabilities and other disturbances associated with the water flow were controlled. For Δt varying between 10 and 30 seconds, 200 hours of simulation time were performed in approximately 1 minute.

In the water flow calibration process the Manning roughness coefficients η were adjusted and the discharge coefficients in bridges and culverts were specified. In valley cells η varied between 0.1 - 0.15 $m^{-1/3}s$, while in main river cells η varied between 0.035 - 0.05 $m^{-1/3}s$ and in ephemeral channels η varied between 0.04 - 0.06 $m^{-1/3}s$. Discharge coefficients in bridges and culverts varied between 0.6 - 0.9.

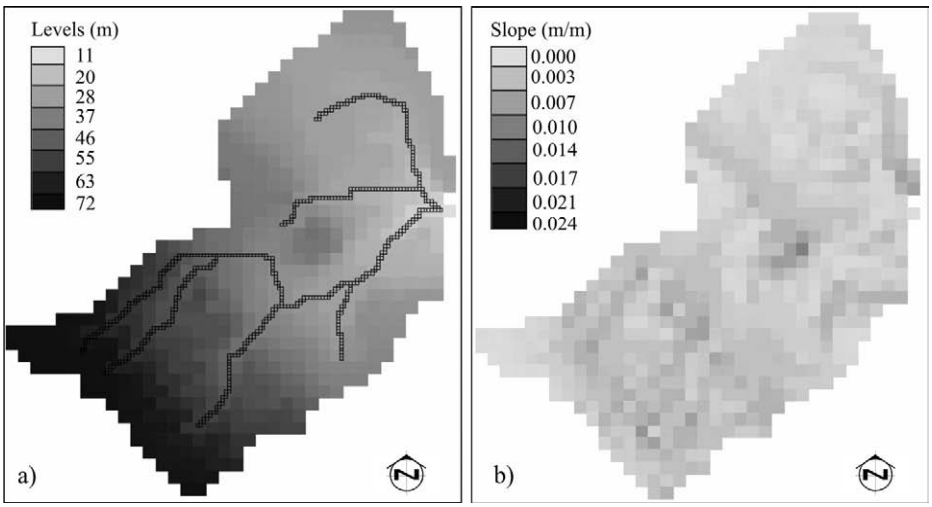

Fig. 5 Model constitution. a) basin discretization and topography for 1,000 m squared grid-size b) spatial distribution of local slopes.

Figure 6 shows the calculated hydrographs at Circunvalación Bridge and Golf Club, together with the observed hydrographs for the event of April 03, 1994. The Nash-Sutcliffe coefficient calculated at Circunvalación Bridge was equal to 0.888. The limnigraph at Golf Club, due to a malfunction, just recorded the final part of the flood. The recession part of the calculated hydrograph at Circunvalación Bridge is steeper than the observed one, which is directly attributed to the uncertainty about the actual mechanisms of storage at subgrid scale. However, considering the level of detail adopted, model results are very satisfactory.

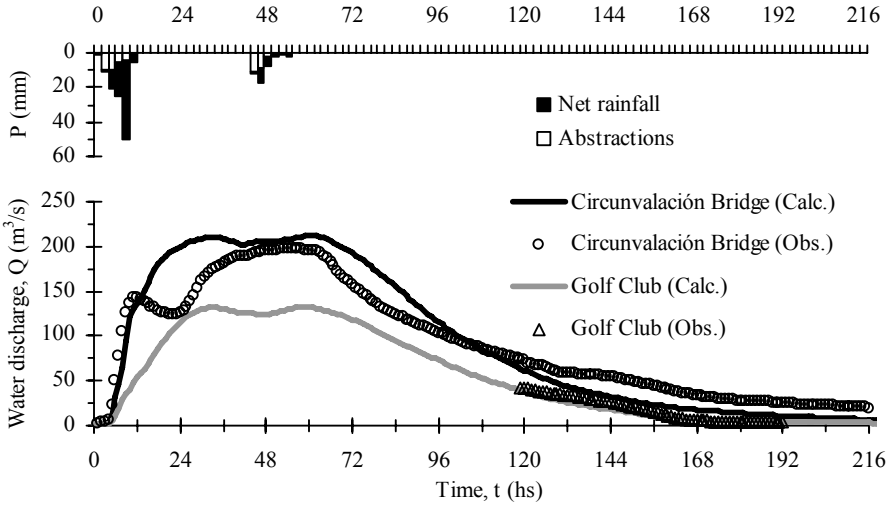

Fig. 6 Calculated and observed hydrographs at Circunvalación Bridge and Golf Club; April 03, 1994

The coefficients c_p (raindrop impact soil erodability), c_f (overland flow soil erodability) and c_t (sediment transport capacity) are the parameters that control sediment yield and transport in the model. For the modeled event no measurements of sediment concentration in any section of the creek were available. Therefore, a sensitivity analysis of the model to variation of those coefficients was made. The ranges of variation of sediment parameters c_p and c_f were specified according to the values suggested in the literature, depending on the textural characteristics of the soil (Meyer and Harmond, 1984; Wicks and

Bathurst, 1996). Soil map of the basin was constructed using soil information published by the National Institute of Agricultural Technology (INTA, Argentina). The topsoils in the basin are classified as silty-loam with a very narrow variation in its composition, as a consequence, the average soil composition for the whole basin was specified, that is, 0.06 (very fine sand fraction), 0.21 (clay fraction) and 0.73 (silt fraction).

Keeping unchanged rainfall input and the corresponding calibrated flow parameters, a number of simulations for different sediment parameters were performed. Particularly, to analyze the influence in sediment yield of coefficients c_t, c_p and c_f, as well as, the total effective surface cover (R_{ac}); four simulations sets were performed. In Table 1 the values of those parameters for each simulation set are presented.

Table 1 Sediment parameters (c_p, c_f, c_t) and R_{ac} for each simulation set

Simulation Set	Total runs	c_t ($m^{-1/2}s$)	c_p $(kg\ m^2s^{-2})^{-1}$	$c_f \times 10^{-6}$ ($kg\ s^{-1}m^{-2}$)	R_{ac} (-)
A	10	0.001 – 0.009	17	2.5	0.65
B	10	0.002	15 - 40	2.5	0.65
C	10	0.002	17	0.5 – 20	0.65
D	10	0.002	17	2.5	0 – 0.9

In addition, for all the model runs the following parameters were set equal to: s=1.65, p=0.5, τ_{bc}=2.45 N/m^2, τ_{ce}=0.6 N/m^2, τ_{cd}=0.08 N/m^2, E=1.3×10^{-8} m/s, θ=0.95, ν=1.01×10^{-6} m^2/s, g=9.81 m/s^2 and the exponents in the sediment transport formula were set equal to: z=1.7, x=1.65, y=0.7, w=1 and r=0.3.

In Fig. 7 the ten runs of simulation set A are presented in terms of sediment delivery ratio (SDR) and the ratio between peak sediment transport rates (RQsp) as function of c_t. It is observed that as c_t is increased, both SDR and peak output sediment transport rate increases. This is because the gross sediment yield is equal for all runs (c_p, c_f and R_{ac} are constants) while sediment transport capacity by overland flow is being increased.

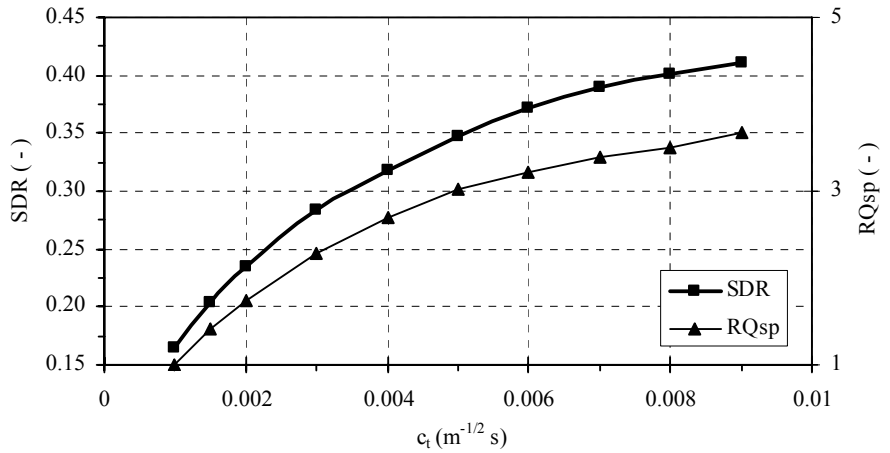

Fig. 7 Sediment delivery ratio SDR and RQsp at Circunvalación Bridge as a function of c_t

In Fig. 8 the ten runs of simulation set B are presented in terms of SDR and RQsp as function of c_p. It is noted that an augment of gross sediment yield associated with raindrop impact (increased c_p) and equal sediment transport capacity (c_t constant) makes SDR to decrease, even when it is observed an increase in the peak output sediment transport rate and consequently an increase in the net sediment yield.

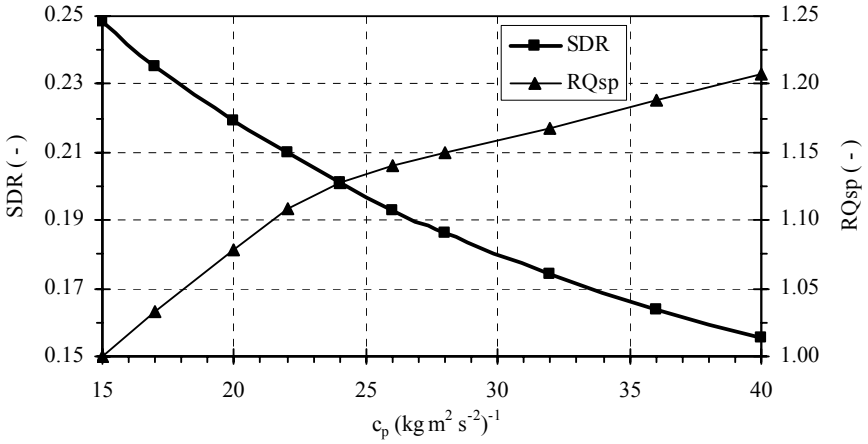

Fig. 8 Sediment delivery ratio SDR and RQsp at Circunvalación Bridge as a function of c_p

In Fig. 9 the ten runs of simulation set C are presented in terms of SDR and RQsp as function of c_f. It is noted that the influence of soil detachment by overland flow in both the gross sediment yield and peak sediment transport rates is similar to that associated to soil detachment by raindrop impact. However, in the case of increment of soil detachment by raindrop impact the corresponding increment of the peak sediment transport rate is greater (Fig. 8).

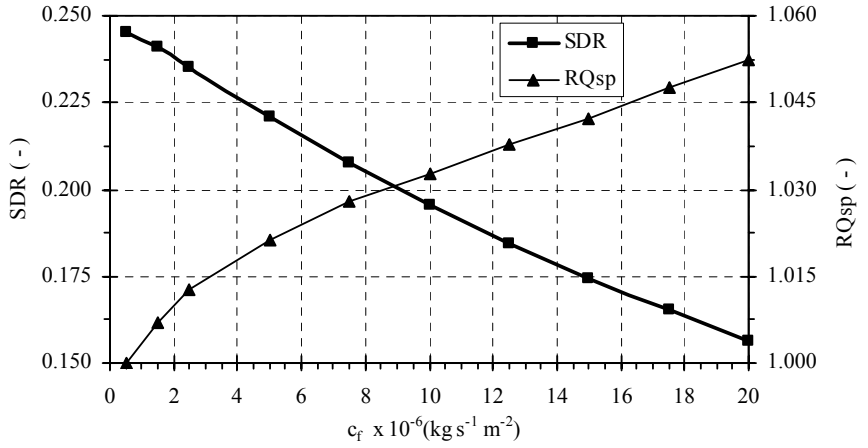

Fig. 9 Sediment delivery ratio SDR and RQsp at Circunvalación Bridge as a function of c_f

In Fig. 10 the ten runs of simulation set D are presented in terms of SDR and RQsp as function of R_{ac}. It is observed that as effective surface cover is increased the peak output sediment transport rate (and the associated net sediment yield) decreases. Moreover, due to an increased soil protection, the SDR increases because the gross sediment yield is reduced to a greater extent than the net sediment yield. In any case, it is clear the important role played by the total effective surface cover (canopy and ground cover) in reducing soil erosion (Wang et al., 2008). For example, the no-till farming system, that leaves stubble as ground cover, protects the soil surface from the direct impact of raindrops and therefore reduces soil erosion processes.

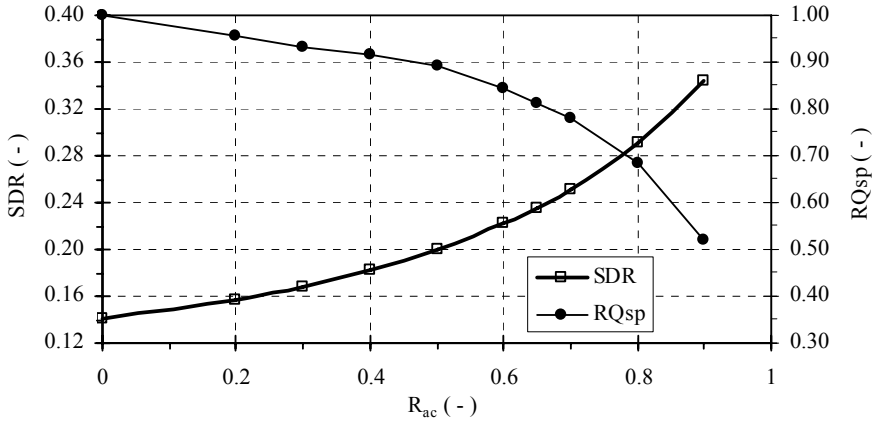

Fig. 10 Sediment delivery ratio SDR and RQsp at Circunvalación Bridge as a function of R_{ac}

According to the predominant cropping of soybean in almost the entire basin, plant development stage and tillage practices at the date of the event, R_{ac} can be estimated equal to 0.65 (Alberts et al., 1995). Moreover, the most plausible values of the sediment parameters corresponds to those of simulation set A run 3 (SAR3): c_t=0.002 ($m^{-1/2}s$), c_p=17 (kg $m^2s^{-2})^{-1}$ and c_f=2.5×10^{-6} (kg $s^{-1}m^{-2}$). In this case, the calculated gross sediment production is 235,068 ton, with an internal re-deposition of about 179,739 ton, then, the net sediment yield is 55,329 ton, that is, approximately 1.8 times greater than the mean annual net sediment yield (Basile et al., 2008), which is possible considering that the simulated event is an extraordinary flooding. The corresponding sediment delivery ratio for the entire hydrological system is SDR=0.235. In Fig. 11 the calculated hydrograph at Circunvalación Bridge together with the temporal distribution of the calculated net sediment yield (sedigraph) for SAR3 are presented. The peak sediment transport is approximately 300 kg/s and the average concentration associated with the whole event, calculated as a function of the total net sediment yield and the volume of the hydrograph, is 733 ppm by weight.

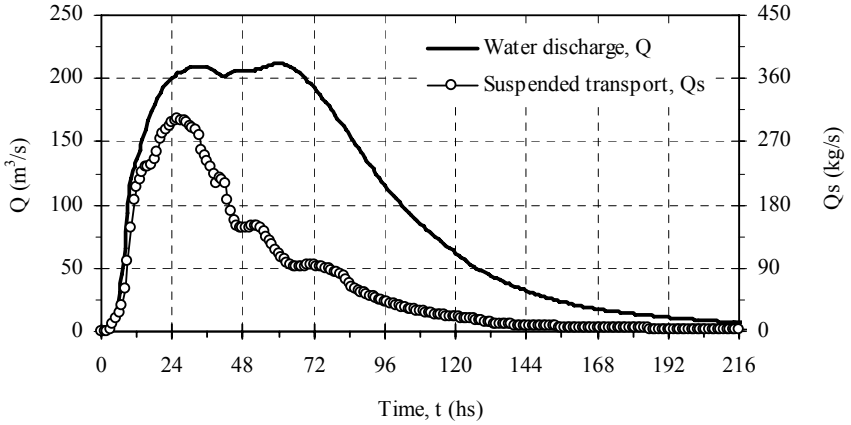

Fig. 11 Calculated hydrograph and sedigraph of Ludueña Creek at Circunvalación Bridge; April 3, 1994. SAR3

Figure 12 shows the calculated hydrograph at Golf Club station and the corresponding sedigraph for simulation SAR3, which distributes in time approximately 34,958 ton of sediment (net sediment yield) and whose peak reaches 235 kg/s. The sediment yield at Golf Club station represents the 63% of the net sediment yield at Circunvalación Bridge and can be associated to an average sediment concentration of 463 ppm by weight for the whole event. Moreover, the net input of sediment from the Ibarlucea channel is 20,372 ton, which represents the remaining 37% of the net sediment input at Circunvalación Bridge.

For this event, similar percentage of distribution and sediment yield amounts have been identified in earlier predictions made with a semi-empirical model (Basile et al., 2007).

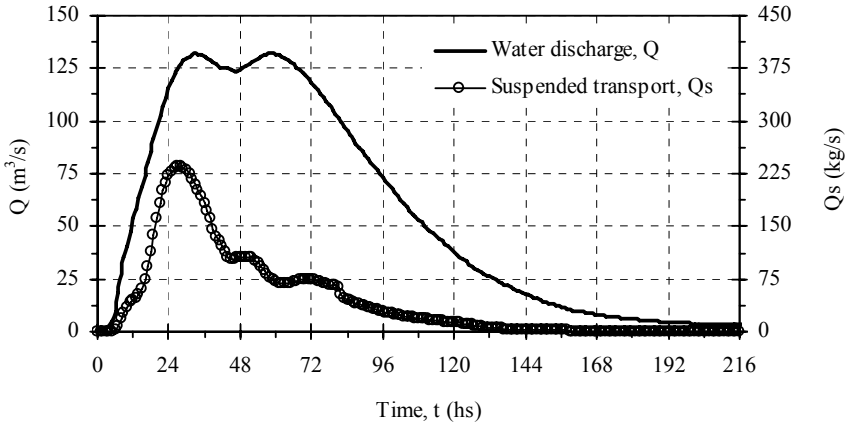

Fig. 12 Calculated hydrograph and sedigraph of Ludueña Creek at Golf Club; April 3, 1994. SAR3

4.3 Model simulation II: Event of March 2007

An extraordinary storm event occurred from the 26th to the 30th March, 2007, in the Ludueña Creek basin. To simulate the flood event and the erosion-sedimentation processes, rainfall data measured at the stations of Rosario Airport, National Load Dispatch (DNC) and Ibarlucea were used. In addition, water discharge and sediment concentration at Circunvalación Bridge were measured during the event. The total precipitation measured at Rosario Airport station was 365 mm, and the average net rainfall over the entire basin was 155 mm. A double peak hydrograph at Circunvalación Bridge was observed. The first peak water discharge was equal to 150 m^3/s and the second one approximately 250 m^3/s.

The DEM and geometric characteristics of man-made structures were updated and incorporated in the model. After different widening works of existing channels, performed by the Water Authority of Santa Fe Province between 1994 and 2007, the dimensions of approximately one hundred culverts, bridges and channels cross sections were updated. Moreover, new culverts, man-made channels and the flood detention dam were incorporated into the model. The entire hydrographic network was also updated with new topographic data obtained from a detailed topographic survey of approximately three hundred cross sections conducted along of approximately 300 km of permanent channels, ephemeral channels and ditches, that is, one cross section per kilometer in average. The spatial discretization of the basin was maintained with squared grid-size cells of 1,000 m. Lateral slope *ITA* and minimum bottom width W_{min} were set equal to 0.009 and 0.10 m respectively, while Manning roughness coefficients and discharge coefficients were varied in a range similar to that set in the event of April 03, 1994.

Since the early 90´s an important change in the crop implantation practices was observed. In fact, in 2007 over 90% of the basin area was sown under no-till cultivation practice (almost 10% in 1994). Therefore, considering a soybean canopy cover of 0.65 and ground cover due to wheat stubble of 0.5, the effective surface cover was estimated equal to R_{ac}= 0.8. Furthermore, sediment coefficients c_p and c_t were set equal to c_p=17 (kg $m^2s^{-2})^{-1}$and c_f=2.5×10^{-6} (kg $s^{-1}m^{-2}$), while c_t was adjusted to reproduce suspended sediment measurements at Circunvalación Bridge. The remaining sediment and numerical scheme parameters were kept unchanged. Figure 13 shows the comparison between calculated and observed hydrographs at Circunvalación Bridge, together with the comparison between calculated and observed suspended sediment transport for the event of March 26, 2007. In Fig. 13 the calculated sedigraph, for c_t=0.002 ($m^{-1/2}$s), shows a first peak approximately of 165 kg/s and a second peak of approximately 298 kg/s. The net sediment yield calculated at Circunvalación Bridge was about 58,700 ton. Model results are quite satisfactory. In fact, it is observed a good agreement between calculated and observed flow and sediment load, the calculated Nash-Sutcliffe coefficient was equal to 0.862 for water discharge and 0.683 for suspended sediment transport. In any case, this is only a comparison at the basin outlet. Sediment eroded somewhere inside the basin will be deposited further downstream. In order to show what happens to the sediment processes within the basin an erosion/deposition map was constructed.

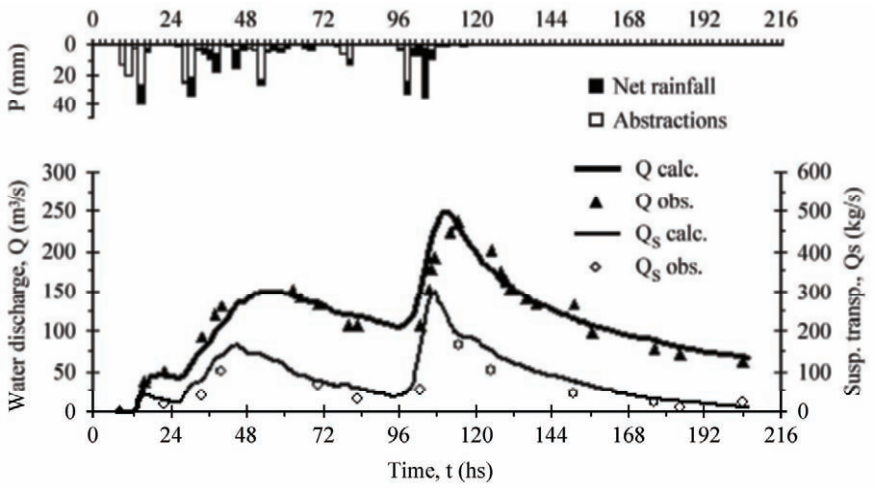

Fig. 13 Calculated and observed water discharge and suspended transport at Circunvalación Bridge; March 26, 2007

Figure 14 shows the spatial distribution of net erosion/deposition processes within the basin. The map was constructed by defining net erosion (negative) / deposition (positive) as the difference between the final accumulated sediment volume in the j-th cell and the corresponding time integral of total gross sediment yield. Areas of net deposition are generally located upstream of culverts, bridges, detention ponds and low gradient cells. Maximum net erosion was calculated in areas of strong concentrated flow like for example downstream of culverts.

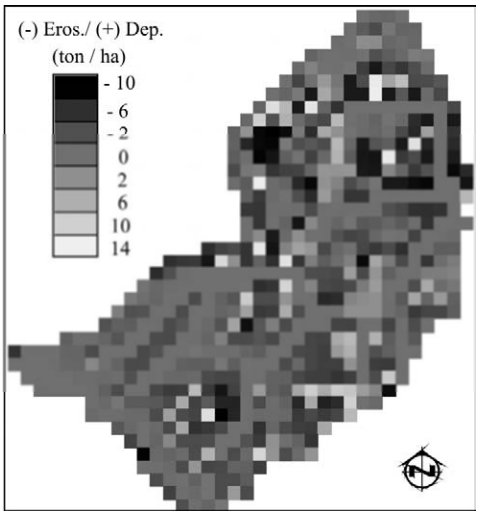

Fig. 14 Net Erosion / Deposition map of Ludueña Creek watershed; March 26, 2007

A more detailed assessment of the spatial distribution of sediment processes in the watershed was carried out by performing a frequency analysis in terms of number of cells (or area) between a given class interval of net erosion/deposition. The class interval of net erosion-deposition was adopted equal to ±0.5 ton/ha. The net erosion shows a maximum value of -9.91 ton/ha, a minimum value of -0.58×10^{-4} ton/ha, an average of -2.75 ton/ha with a standard deviation of 2.63 ton/ha. On the other hand, the net deposition shows a maximum value of 13.75 ton/ha, a minimum value of 2.08×10^{-4} ton/ha, an average of 3.45 ton/ha with a

standard deviation of 3.73 ton/ha. Figure 15 shows the relative and cumulated frequency curves. From the cumulated frequency curve it is observed that approximately 74% of the area was affected by erosion while the remaining 26% by sedimentation. Moreover, about 46% of the cells undergo a net erosion between the minimum value of -0.58×10^{-4} ton/ha and the mean value of -2.75 ton/ha.

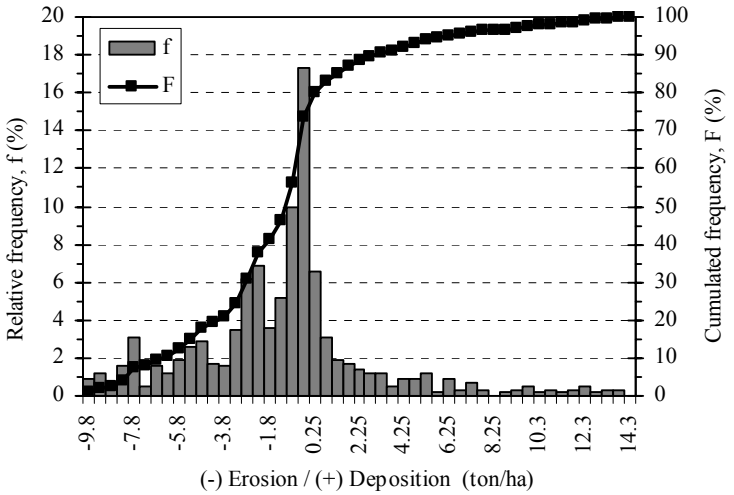

Fig. 15 Frequency analysis of net Erosion / Deposition, Ludueña Creek watershed; March 26, 2007

5 Conclusions

The physically-based model CTSS8-SED presented in the paper is suitable for simulating storm runoff and the associated erosion-sedimentation processes in lowland basins. The reliability of sediment transport calculations rests on an accurate description of the runoff process. Many watershed-hydrology and sediment yield models represents the dynamics of runoff in a simplified form through the implementation of one-dimensional flood routing models, like hydrologic or kinematic wave routing. Such representation of flow propagation processes are not adequate for the overland and stream flow in lowland basins where the flow is conditioned by road and railways embankments interferences. In fact, this approach does not allow the transmission of hydrodynamic information upstream, furthermore, in many situations the one-dimensional runoff assumption is not representative of the real runoff pattern. Indeed, simulations have shown that, during extraordinary rainfalls events, structures such as bridges and culverts produce backwater effects that affect flow variables up to considerable distances upstream. Moreover, the runoff dynamics in the valley areas shows predominantly two-dimensional features and the flow is driven by hydraulic gradient rather than by topographic gradient. The model has successfully reproduced the observed hydrographs during the simulated events in the Ludueña Creek basin. Also, spatially-distributed flow parameters calculated with the model provide for the adequate evaluation of raindrop impact detachment, overland flow detachment and sediment routing in the basin.

Acknowledgements

The authors would like acknowledge the financial support provided by the National Council of Scientific and Technical Research (CONICET) and the National Agency for Science and Technology Promotion (ANPCYT) of Argentina trough the projects PIP 5308 and PICTO 23187, respectively. We wish to thank also Professor Giampaolo Di Silvio for his constructive comments.

References

Alberts E. E., Nearing M. A., Weltz M. A., Risse L. M., Pierson F. B., Zhang X. C., Laflen J. M., and Simanton J. R. 1995, Soil component. USDA-Water Erosion Prediction Project: Hillslope Profile and Watershed Model Documentation. Chapter 7, pp. 7.1–7.45. Rep. No. 10. USDA-ARS National Soil Erosion Research Laboratory, West Lafayette, IN.

Ariathurai R. and Arulanandan K. 1978, Erosion rate of cohesive soils. Journal of Hydr. Engineering, Vol. 104, No. 2, pp. 279–283.

Arnold J. G., Williams J. R., Nicks A. D., and Sammons N. B. 1989, SWRRB, a basin scale simulation model for soil and water resources management. Texas A&M Press, College Station, Texas, USA.
Arnold J. G., Srinivasan R., Muttiah R. S., and Williams J. R. 1998, Large-area hydrologic modeling and assessment: Part I. Model development. Journal of American Water Resources Association, Vol. 34, No. 1, pp. 73–89.
Basile P. A. 2007, Sediment modules coupled to the quasi-2D physically-based and spatially-distributed CTSS8 model (in Spanish). Technical Report I0207. Department of Hydraulics. National University of Rosario.
Basile P. A., Riccardi G., and Stenta H. 2008, Development and application of model EROSUP-U for mean annual sediment yield assessment at basin scale (in Spanish). In: G. Riccardi, P.A.Basile, E.D. Zimmermann, H. Stenta, C. Scuderi, J. Rentería and M. Garcia (Eds.). Modelling hydrological processes in lowland areas, ISBN 978-950-673-691-0, UNR Press, Rosario, Argentina, pp. 199–215.
Basile P. A., Riccardi G., Stenta H., and Garcia M. 2005, Evaluation of erosion/sedimentation processes in the Ludueña Creek basin (in Spanish). II Regional Symposium on Rivers Hydraulics, Neuquén, Argentina.
Basile P. A, Riccardi G., Stenta H., and Zimmermann E. 2007, Water and sediment yield simulation at basin scale by coupling a hydrologic-hydraulic model with MUSLE (in Spanish). XXI National Water Congress, Tucumán, Argentina.
Beasley D. B., Huggings L. F., and Monke E. J. 1980, ANSWERS: A model for watershed planning. Transactions of the Am. Soc. of Agric. Engns., Vol. 23, No. 4, pp. 938–944.
Bingner R. L. and Theurer F. D. 2001, AnnAGNPS Technical Processes: Documentation Version 2.
Borah D.K. and Bera M. 2003, Watershed-scale hydrologic and nonpoint-source pollution models review of mathematical bases. Transactions of the ASAE, Vol. 46, No. 6, pp. 1553–1566.
Bouraoui F. and Dillaha T. A. 1996, ANSWERS-2000: Runoff and sediment transport model. Journal of Environmental Engineering, Vol. 122, No. 6, pp. 493–502.
Casas R. 2003, Sustainability of agriculture in the Pampean region (in Spanish). Technical report. National Institute for Agriculture Technology (INTA). Climate and Water Division. Castelar, Argentina.
Ching-Nuo Chen, Tsai Chih-Heng, and Tsai Chang-Tai. 2006, Simulation of sediment yield from watershed by physiographic soil erosion-deposition model. Journal of Hydrology (2006), 327, pp. 293–303.
Chow Ven Te. 1959, Open-channel hydraulics. McGraw Hill, New York, USA.
Chow Ven Te, D. R. Maidment, and L.W. Mays. 1994, Applied Hydrology (in Spanish). McGraw Hill Interamericana S.A. ISBN 958-600-171-7.
Clark E. H. 1985, The off-site costs of soil erosion. Journal of Soil and Water Conservation. 40, pp. 19–22.
Crosson P. 1997, Will erosion threaten agricultural productivity? Environment 39, pp. 4–5.
Cunge J. 1975, Two Dimensional Modelling of Flood Plains. Chapter 17: Unsteady flow in open channels. K. Mahmood and V. Yevjevich (Eds.) 1975. Water Resources Publications, Fort Collins, USA.
Cunge J. A, Holly F. M., and Verwey A. 1980, Practical Aspects of Computational River Hydraulics. Pitman, London.
De Roo A. P. J., Wesseling C. G., and Ritsema C. J. 1996, LISEM: A single-event physically-based hydrological and soil erosion model for drainage basins. I: Theory, input and output. Hydrological Processes, 10, pp. 1107–1117.
Di Silvio G. 1983, Mathematical models for short and long-term simulation of morphological river bed changes (in Italian). Studies and Researches Nº 356, University of Padua, Padua, Italy.
Engelund F. and Hansen A. 1967, A monograph on sediment transport in alluvial streams. Tech. Univ. of Denmark.
Ewen J., Parkin G., and O´Connell P. E. 2000, SHETRAN: Distributed river basin flow and transport modeling system. ASCE, Journal of Hydrologic Engineering, 5.
Foster G. R. and Lane L. J. 1987, User requirements UDSA-Water Erosion Prediction Project (WEPP). NSERL Report Nº 1, USDA-ARS National Soil Erosion Research Laboratory, West Lafayette, IN., 43 p.
Heppner C. S., Ran Q., VanderKwaak J. E., and Loague K. 2005, Adding sediment transport to the integrated hydrology model (InHM): Development and testing. Advances in Water Resources, 29 (2006) 930-943. Available on line October 13, 2005.
Julien P. and Rojas R. 2002, Upland erosion modeling with CASC2D-SED. International Journal of Sediment Research, ISSN 1001-6279, Vol. 17, No. 4, pp. 265–274.
Khosronejad A. 2009, Optimization of the Sefid-Roud dam desiltation process using a sophisticated one-dimensional numerical model. International Journal of Sediment Research, Vol. 24, No. 2, pp. 189–200.
Krone R. B., Ariathurai R., and MacArthur R. 1977, Mathematical model of estuarial sediment transport. Technical report D-77-12, USACE, Dredged Material Research Program, Vicksburg, Mississipi, USA.
Laflen J. M., Elliot W. J., Simanton R., Holzhey S., and Kohl K. D. 1991, WEPP soil erodibility experiments for rangeland and cropland soils. Journal of Soil and Water Conservation, 46, pp. 39–44.
Lane L. J., Shirley E. D., and Singh V. P. 1988, Modelling erosion on Hillslope. Chapter 10 Modelling Geomorphological Systems. Edited by M. G. Anderson. 1988 John Wiley & Sons Ltd.
Meyer L. D. and Harmond W. C. 1984, Susceptibility of agricultural soils to interrill erosion. Soil Science Society American Journal, 48, pp. 1152–1157.

Morgan R. P. C., Quinton J. C., Smith R. E., Govers G., Poesen J. W. A., Auerswald K., Chisci G., Torri D., and Styczen M. E. 1998, The European Soil Erosion Model (EUROSEM): a dynamic approach for predicting sediment transport from fields and small catchments. Earth Surface Processes and Landforms, 23, pp. 527–544.

Moscatelli G. and Pazos M. S. 2000, Soils of Argentina: Nature and Use. In: I. Kheoruenromne and S. Theerawong (Eds.) 2000. Proceedings of International Symposium on Soil Science: Accomplishments and Changing Paradigm towards the 21st Century, Bangkok, Thailand. ISBN 974-87749-4-5, pp. 81–92.

Nearing M. A., Bradford J. M., and Parker S. C. 1991, Soil detachment by shallow flow at low slopes. Soil Science Society American Journal, 55, pp. 339–344.

Nunes J. P., Vieira G. N., and Seixas J. 2005, MEFIDIS – A physically-based, spatially-distributed runoff and erosion model for extreme rainfall events. In: Singh, V.P., Frevert, D.K. (Eds.), Watershed Models. CRC Press, Boca Raton, pp. 291–314.

Nunes J. P., de Lima J. L. M. P., Singh V. P., de Lima M. I. P., and Vieira G. N. 2006, Numerical modeling of surface runoff and erosion due to moving rainstorms at the drainage basin scale. Journal of Hydrology (2006) 330, pp. 709–720.

Oldeman L. R. 2000, Impact of soil degradation: a global scenario. Proceedings of International Conference of Managing Natural Resources for Sustainable Agricultural Production in the 21st Century. New Delhi, Feb. 2000.

Park S. W., Mitchell J. K., and Scarborough J. N. 1982, Soil erosion simulation on small watershed: a modified ANSWER model. Transactions ASAE 25, pp. 1581–1588.

Pimentel D., Harvey C., Resosudarmo P., Sinclair K., Kurz D., McNair M., Crist S., Shpritz L., Fitton L., Saffouri R., and Blair R. 1995, Environmental and economic costs of soil erosion and conservation benefits. Science 267, pp. 1117–1123.

Renard, K. G.; Foster G. R.; Weesies G. A., and Porter J. P. 1991, RUSLE: Revised universal soil loss equation. J. Soil Water Conserv, Vol. 46, No. 1, pp. 30–33.

Riccardi G. A. 2000, A Quasi-2D Hydrologic-Hydraulic Modeling System for Rural and Urban Environments (in Spanish). PhD Thesis, National University of Cordoba, Argentina.

Riccardi G. A.; Basile P. A.; Stenta H.; Riesco G., and Baglietto P. 2005, Regional adjustment of erosion predictors in cohesive soils (in Spanish). XX National Water Congress, Mendoza, Argentina. CD-Rom ISBN: 9872214301.

Singh V. P. and Woolisher D. A. 2002, Mathematical modeling of watershed hydrology. Journal of Hydrologic Engineering, ISSN 1084-0699, Vol. 7, No. 4, pp. 270–292.

Steegen A., Govers Takken G., L., Nachtergaele J., Poesen J., and Merckx R. 2001, Factors controlling sediment and phosphorous export from two Belgian agricultural catchments. Journal of Environmental Quality 30, pp. 1249–1258.

Stenta H., Rentería J. P., and Riccardi G. A. 2005, Computational platform for information management in surface runoff simulation (in Spanish). XX National Water Congress, Mendoza, Argentina. CD-Rom ISBN: 9872214301.

Sun H., Cornish P. S., and Daniell T. M.. 2002, Contour-based digital elevation modeling of watershed erosion and sedimentation: Erosion and sedimentation estimation tool (EROSET). Water Resources Research, Vol. 38, No. 11, pp. 1-10.

UMSEF 2007, Monitoring native forests in Argentina. Period 1998–2006 (in Spanish). Management Unit of Forestry Evaluation System (UMSEF). Forest Division. Secretary of Environment and Sustainable Development. June 2007, Argentina.

Verstraeten G. and Poesen J. 1998, Flooding of properties and sedimentation in retention ponds in central Belgium. In Modelling Soil Erosion, Sediment Transport and Closely Related Hydrological Processes. IAHS Publication Nº 249, pp. 187–194.

Walling, D. E and Quine T. A. 1991, Recent rates of soil loss from areas of arable cultivation in the UK. In Sediment and Stream Water Quality in a Changing Environment: Trends and Explanation. N.E. Peters and D.E. Walling (Eds.) IAHS Publication Nº 203, pp. 123–132.

Wang Z., Wang G., and Huang G. 2008, Modeling of state of vegetation and soil erosion over large areas. International Journal of Sediment Research, Vol. 23, No. 3, pp. 181–196.

Wang Z. and Hu Ch. 2009, Strategies for managing reservoir sedimentation. International Journal of Sediment Research, Vol. 24, No. 4, pp. 369–384.

Wicks J. M, Bathurst J. C., Johnson C. W., and Ward T. J. 1988, Application of two physically-based sediment yield models to plot and field scale. IAHS Publication Nº 174, pp. 583–591.

Wicks J. M. and Bathurst J. C. 1996, SHESED: A physically-based, distributed erosion and sediment yields component for the SHE hydrological modelling system. Journal of Hydrology (1996), 175, pp. 213–238.

Wischmeier W. H. and Smith D. D. 1978, Predicting rainfall erosion losses – a guide for conservation planning. U.S. Department of Agriculture, Agriculture Handbook Nº 537.

Woolisher D. A.; Smith R. E., and Goodrich D. C. 1990, KINEROS, A Kinematic Runoff and Erosion Model: Documentation and User Manual. USDA, Agric. Research Service, Rep. ARS-77, Fort Collins, Colorado.

Yi Y., Wang Z., Zhang K., Yu G., and Duan X. 2008, Sediment pollution and its effect on fish through food chain in the Yangtze River. International Journal of Sediment Research, Vol. 23, No. 4, pp. 338–347.

Young R. A.; Onstad A., Bosch D., and Anderson P. 1987, AGNPS, Agricultural nonpoint-source pollution model: A watershed analytical tool. USDA, Conservation Research Report Nº 35.
Zhang G. H., Liu B. Y., Liu G. B., He X. W., and M. A. Nearing. 2003, Detachment of undisturbed soil by shallow flow. Soil Science Society American Journal 67, pp. 713–719.
Zhou W. and Wu B. 2008, Assessment of soil erosion and sediment delivery ratio using remote sensing and GIS: A case study of upstream Chaobaihe river catchment, North China. International Journal of Sediment Research, Vol. 23, No. 2, pp. 167–173.
Zimmermann E. D. and Basile P. A. 2008, Pedotransfer functions for silty-loam soils (in Spanish). In: Riccardi G., Basile P. A., Zimmermann E. D., Stenta H., Scuderi C., Rentería J. and Garcia M. (Eds.). Modelling hydrological processes in lowland areas, ISBN 978–950–673–691–0, UNR Press, Rosario, Argentina, pp. 133–144.